



Published in final edited form as:

*JAMA Ophthalmol.* 2013 October ; 131(10): 1267–1274. doi:10.1001/jamaophthalmol.2013.4321.

## Analysis of Morphological Features and Vascular Layers of Choroid in Diabetic Retinopathy Using Spectral-Domain Optical Coherence Tomography

Mehreen Adhi, MBBS<sup>1,2</sup>, Erika Brewer<sup>2</sup>, Nadia K Waheed, MD, MPH<sup>1,2</sup>, and Jay S. Duker, MD<sup>1,2</sup>

<sup>1</sup>New England Eye Center, Tufts Medical Center, Boston, Massachusetts, USA

<sup>2</sup>Tufts University School of Medicine, Boston, Massachusetts, USA

### Abstract

**Importance**—Diabetic retinopathy (DR) is characterized by microaneurysms, capillary nonperfusion, and ischemia within the retina, ultimately leading to neovascularization and/or macular edema. Evidence suggests that choroidal angiopathy may coexist with retinal vascular damage. Recent advances in spectral-domain optical coherence tomography (SD-OCT) permit an efficient visualization of the choroid.

**Objective**—To analyze the morphological features and vascular layers of the choroid in patients with DR using SD-OCT.

**Design**—A cross-sectional retrospective review identified patients with DR and healthy (control) subjects who underwent 1-line raster scanning from February 1, 2010, through June 30, 2012. Patients were classified into the following 3 groups: nonproliferative DR without macular edema (9 eyes), proliferative DR without macular edema (PDR) (10 eyes), and diabetic macular edema (DME) (14 eyes). Two independent raters experienced in analyzing OCT images evaluated the morphological features and vasculature of the choroid.

**Setting**—New England Eye Center.

**Participants**—Thirty-three eyes of 33 patients with DR and 24 eyes of 24 controls.

**Exposure**—Diabetic retinopathy.

**Main outcome and measure**—Choroidal morphological features and vasculature analysis.

**Results**—The choroidoscleral interface had an irregular contour in 8 of 9 eyes with nonproliferative DR (89%), 9 of 10 eyes with PDR (90%), and 13 of 14 eyes with DME (93%) compared with 0 of 24 controls. The thickest point of the choroid was displaced from under the fovea, and focal choroidal thinning was observed in eyes with DR. Mean subfoveal choroidal thickness and mean subfoveal medium choroidal vessel layer and choriocapillaris layer thickness were significantly reduced in eyes with PDR ( $P < .05$ ) and DME ( $P < .05$ ) compared with controls.

---

**Corresponding Author/Reprint Requests:** Jay S. Duker, MD New England Eye Center Tufts Medical Center 800 Washington Street, Boston, MA 02111 Phone: 617-636-4677 Fax: 617-636-4866 Jduker@tuftsmedicalcenter.org.

**Financial Interest Disclosures** Jay S. Duker receives research support from Carl Zeiss Meditech, Inc. and Optovue, Inc..

**Conclusions and relevance**—Choroidal morphological features are altered in patients with moderate to severe DR. The subfoveal choroidal thickness and the subfoveal medium choroidal vessel layer and choriocapillaris layer thicknesses are significantly reduced in patients with PDR and DME. To our knowledge, this is the first study to analyze the morphological features and vasculature of the choroid in DR using SD-OCT. These findings may be clinically useful in predicting the progression of DR.

---

## INTRODUCTION

Diabetic retinopathy (DR) is the leading cause of visual impairment in working-age adults worldwide. The disease is characterized by microaneurysms, capillary nonperfusion, and ischemia within the retina, ultimately leading to neovascularization and/or macular edema, both of which can severely compromise visual function (1).

The pathogenesis and clinical features of DR are primarily attributed to retinal vascular damage; however, evidence suggests that choroidal angiopathy may coexist. Delayed choroidal vascular filling, which appears as choroidal hypofluorescence on indocyanine green angiography (2-4), has been demonstrated in the eyes of humans with diabetes mellitus and shown to correlate with the severity of DR (2,5-8). Laser Doppler flowmetry studies show a reduction in choroidal blood flow and volume in patients with nonproliferative (NPDR) and proliferative DR (PDR) (9). In addition, histological studies reveal choroidal vascular degeneration, choroidal aneurysms, choroidal neovascularization, choriocapillaris “dropout” (a nonperfusion and/or a complete attenuation of the choriocapillaris), and increased tortuosity and narrowing of the choroidal vessels in eyes with DR (6,10).

Recent advances in spectral-domain optical coherence tomography (SD-OCT) permit an efficient visualization of the choroid up to the choroidoscleral interface. These advances include better penetration, higher acquisition speed, 3-dimensional imaging, image averaging, and resolution to a micrometer scale (11,12). Studies using SD-OCT reveal changes in choroidal thickness in healthy and pathologic states (13-20). Although SD-OCT–detected changes in choroidal thickness in patients with DR have been described previously (20), to our knowledge, an analysis of the morphological features and the vascular layers of the choroid in eyes with DR by using SD-OCT has not been performed to date.

The choroid provides oxygen and nutrients to the outer third of the retina and consists of the following 3 vascular layers: the choriocapillaris layer, the choroidal layer composed of medium-sized vessels (Sattler layer), and the large-vessel choroidal layer (Haller layer) (21-23). Given that the choroid is involved in many diseases of the posterior segment, an analysis of changes in its morphological features and vasculature in chorioretinal diseases may be of clinical relevance. In view of the evidence suggesting the presence of choroidal angiopathy in DR (2-10,13-20), this study aimed to characterize the morphological features of the choroid and analyze its vasculature in patients with DR by using SD-OCT.

## METHODS

### Subjects

We identified retrospectively 33 patients with DR (33 eyes) and 24 healthy subjects (24 eyes) who underwent high-definition 1-line raster scanning at the New England Eye Center from February 1, 2010, through June 30, 2012.

Diagnostic criteria for DR were based on an ophthalmic history and complete ophthalmic evaluation, including a dilated fundus examination, fundus photography, OCT imaging, and, in selected cases, fluorescein angiography. Patients with a myopic refractive error of greater than 8 diopters (D), concomitant pathological findings in the posterior segment, prior vitrectomy, and a history of hypertension were excluded. Clinical examination and OCT findings were used to characterize patients into the following 3 groups: NPDR without macular edema (9 eyes), PDR without macular edema (10 eyes), and diabetic macular edema (DME) (14 eyes). The eyes in the NPDR and PDR groups did not have a history of macular edema. All eyes in the PDR group had previously been treated with panretinal photocoagulation. In addition, all eyes in the DME group received previous treatment with focal laser photocoagulation, whereas 8 of 14 DME eyes (57%) received previous treatment with anti-vascular endothelial growth factor (VEGF) agents. Best-corrected visual acuity and automated central retinal thickness measurements generated by the macular cube scan protocol were also collected from the patients' medical records.

The healthy subjects (control group) had a best-corrected visual acuity of 20/20 OU or better, underwent fundus examination and OCT imaging, and had no retinal or choroidal pathological features. Subjects with a myopic refractive error of greater than 8D were excluded. This study was approved by the institutional review board of Tufts Medical Center and is adherent to the tenets of the Declaration of Helsinki.

### SD-OCT Scanning

We performed SD-OCT using a high-definition 1-line raster scanner (Cirrus; Carl Zeiss Meditec Inc). This 6-mm line scan consists of 4096 A scans, an imaging speed of 27 000 A-scans per second, and an axial resolution of approximately 5 $\mu$ m in tissue. The device acquires 20 frames at the same retinal location that are averaged together to increase the signal to noise ratio. This process allows for better visualization of the choroid. The images were not inverted to bring the choroid in closer proximity to the zero-delay line because image inversion using the SD-OCT software results in a low-resolution, pixilated image. The enhanced depth imaging protocol was not used because it was not available on the high-definition SD-OCT device at the time these scans were performed. All scans had an intensity of 6:10 or greater (ratio of signal to noise) and were taken horizontally, as close to the center of the fovea as possible, such that the thinnest point of the macula was imaged in both groups and that any discrepancies in the analysis of the morphological features and vascular layers of the choroid due to slight differences in positioning could be avoided. A single operator trained in acquiring OCT images performed all the imaging. One scan per patient with DR that had a clearly identifiable choroidoscleral interface was used for the purpose of

analysis. For comparison, 1 scan from each subject in the control group was selected randomly for analysis.

### Morphological Features of the Choroid

Two independent raters (M.A. and E.B.) experienced in analyzing OCT images evaluated the choroid for morphological features. The clarity of the choroidoscleral interface was examined throughout the 6-mm line scan owing to its importance in measuring the choroidal thickness. The contour and shape of the choroidoscleral interface was evaluated and labeled as being convex (or bowl shaped) or S shaped (having an irregular or concave-convex-concave shape with >1 inflection point) (Figure 1). We identified the site of the thickest point of the choroid and compared the location of this point with the overlying retina. The location was considered subfoveal when the thickest choroidal point was exactly beneath the foveal center or within 100 $\mu$ m nasal and 100 $\mu$ m temporal to the foveal center. Thus, if the thickest point of the choroid fell within a 200 $\mu$ m (0.2-mm) region beneath and centered on the foveal center, it was considered subfoveal (Figure 2). Areas of focal thinning of the choroid were identified. If abnormal thinning of the choroid was observed, choroidal thickness was measured (as described below) at that location, and eyes were considered to have focal thinning if choroidal thickness at the measured location was 50% less than that of the mean choroidal thickness of normal eyes at the corresponding location. The mean choroidal thickness measurements in healthy eyes reported previously (24) were used as a reference to define focal thinning in eyes with DR.

### Analysis of Choroidal Vasculature

The mean (SD) luminal diameter of large choroidal vessels, including arteries and veins, ranges from 28.2 (11.2) to 37.1 (12.5)  $\mu$ m on histological analysis of healthy eyes (23). However, because histological analysis can lead to alteration of the tissue owing to postmortem changes and processing artifacts (23), a direct correlative investigation of histological features and OCT imaging is not possible. For this reason, a pilot study (25) on OCT images of 42 healthy eyes was performed before choroidal vasculature analysis in this study. Two independent observers (including M.A.) experienced in analyzing OCT images measured the diameter of the smallest visible large vessel located near the choroidoscleral border within the 6-mm region of the 1-line raster scan. We measured the diameters in the nasal temporal plane using the linear measurement tool of the OCT scanner and calculated the mean of the measurements of the 2 observers. The mean diameter of the smallest visible large choroidal vessels in normal eyes was 100 (range, 86-108)  $\mu$ m (unpublished study performed by M.A., Lauren A. Branchini, MD, Caio V. Regatieri, MD, PhD, and J.S.D., March-May 2011) on OCT (25). This diameter was used as a cutoff for defining a large choroidal vessel for choroidal vasculature analysis in the present study. Figure 3 depicts the method used for analysis of the choroidal vascular layers. This method has been described previously (25). First, choroidal thickness beneath the fovea was measured from the outer border of the hyperreflective retinal pigment epithelium to the inner border of the choroidoscleral interface. We selected a large choroidal vessel measuring at least 100 $\mu$ m, located close to the choroidoscleral interface and in the closest proximity to the fovea, and drew a perpendicular line from the innermost point of that vessel, intersecting the choroidal thickness measurement line. We measured the thickness of the subfoveal large choroidal

vessel layer (the Haller layer) perpendicularly from the inner border of the sclera to the intersection point on the choroidal thickness measurement line. This thickness measurement was then subtracted from the total choroidal thickness to obtain the thickness of the medium choroidal vessel layer (the Sattler layer) and choriocapillaris layer. Two independent raters (M.A. and E.B.) experienced in analyzing OCT images performed all the measurements, and the mean measurement of the 2 observers was used for the purpose of analysis. All the vasculature measurements were performed beneath the fovea.

### Statistical Analysis

All data were expressed as mean (SEM). We used 1-way analysis of variance to determine the differences in the subfoveal choroidal thickness, in the subfoveal large choroidal vessel layer thickness, and in the combined thickness of the subfoveal medium choroidal vessel layer and choriocapillaris layer between controls and eyes with DR. We applied the Tukey multiple comparison test to assess these variables in eyes with NPDR, PDR, and DME compared with controls. We used the unpaired t test to determine the difference in all the vasculature measurements in eyes treated with anti-VEGF agents and treatment-naive eyes within the DME group. Pearson product moment correlation was used to determine the interobserver agreement for all the measurements and for the association of subfoveal choroidal vascular measurements with central retinal thickness. A 95% confidence interval and a 5% level of significance were adopted; therefore,  $P < .05$  was considered significant. All statistics were performed using commercially available software (Prism 5.0 software for Macintosh; GraphPad Software, Inc).

## RESULTS

The demographic and clinical characteristics of the patients with DR and control group are depicted in Table 1. We found no significant difference between the mean ages and mean refractive error of DR patients and controls ( $P = .80$  and  $P = .62$ , respectively).

### Choroid Findings

The choroidoscleral interface had an irregular contour in 8 of 9 eyes with NPDR (89%), 9 of 10 eyes with PDR (90%), and 13 of 14 eyes with DME (93%) compared with 0 of 24 controls. All the studied morphological features of the choroid and representative images with illustration of some of the features in eyes with NPDR, PDR, and DME compared with controls are depicted in Table 2 and Figure 2.

The mean subfoveal choroidal thickness, mean subfoveal large choroidal vessel layer thickness, and mean combined subfoveal medium choroidal vessel layer and choriocapillaris layer thickness were significantly reduced in eyes with DR compared with controls (Table 3). As a subgroup, however, eyes with NPDR did not show a significant difference in the mean subfoveal choroidal thickness, mean subfoveal large choroidal vessel layer thickness, and mean combined subfoveal medium choroidal vessel layer and choriocapillaris layer thickness compared with controls ( $P > .05$ ,  $P > .05$ , and  $P > .05$ , respectively) (Figure 4 and Figure 5). In eyes with PDR and DME, we found a significant reduction of the mean subfoveal choroidal thickness ( $P < .05$ ) and the mean combined subfoveal medium choroidal

vessel layer and choriocapillaris layer thickness ( $P < .05$ ) compared with controls (Figures 4 and 5). All measurements had a strong interobserver correlation ( $r = 0.73$  [ $P < .001$ ],  $r = 0.69$  [ $P = .001$ ], and  $r = 0.71$  [ $P < .001$ ]) for subfoveal choroidal thickness, subfoveal large choroidal vessel layer thickness, and combined subfoveal medium choroidal vessel layer and choriocapillaris layer thickness, respectively. The maximum choroidal thickness was subfoveal only in 2 of 9 eyes with NPDR (22%), 2 of 10 eyes with PDR (20%), and 2 of 14 eyes with DME (14%) compared with 23 of 24 controls (96%). Focal thinning of the choroid with respect to the mean choroidal thickness measurements at the corresponding locations in healthy eyes (24) was observed in 5 of 9 eyes with NPDR (56%), 4 of 10 eyes with PDR (40%), and 12 of 14 eyes with DME (86%) compared with 0 of 24 controls. Mean subfoveal choroidal thickness, mean subfoveal large choroidal vessel layer thickness, and mean medium choroidal vessel layer and choriocapillaris layer thickness had no correlation with the central retinal thickness in patients with DR ( $r = 0.2$  [ $P = .31$ ];  $r = 0.15$  [ $P = .12$ ]; and  $r = 0.18$  [ $P = .27$ ], respectively).

The large choroidal vessel layer thickness was significantly reduced in eyes with DR compared with controls ( $P = .04$ ) (Table 3). As a subgroup, however, eyes with NPDR, PDR, and DME did not have a significant thinning of the large choroidal vessel layer compared with controls ( $P > .05$ ) (Figure 5). Within the DME group (14 eyes), eyes that received anti-VEGF therapy (8 of 14 [57%]) had no significant difference in the choroidal thickness and vasculature measurements compared with eyes that did not receive anti-VEGF therapy (6 of 14 [43%]) ( $P = .67$ ), although the number of patients in each group was small.

## DISCUSSION

The present study demonstrates alterations in choroidal morphological features in eyes with DR. In addition, we show a reduction in the total choroidal thickness and the combined thickness of the medium choroidal vessel layer and choriocapillaris layer in eyes with PDR and DME, but not in eyes with less advanced disease (NPDR only), compared with controls. The reduction in the total choroidal thickness in eyes with PDR and DME is consistent with a previous study on choroidal thickness in patients with DR (20). To the best of our knowledge, however, this study is the first to characterize morphological analysis of the choroid and the evaluation of its vascular layers in eyes with DR by using SD-OCT.

Although indocyanine green angiography and laser Doppler flowmetry are conventionally used for evaluation of choroidal vessels and choroidal blood flow, respectively, the advantage of using SD-OCT is its ability to visualize the choroid in vivo with precise anatomic detail. This study demonstrates significant alterations in choroidal morphological features in eyes with advanced DR. These alterations included an irregular or an S shape to the choroidoscleral interface in most DR eyes and a displacement of the thickest point of choroid from under the foveal center. Focal thinning of the choroid in eyes with DR compared with the corresponding locations in healthy eyes (24) was also detected and appeared to correlate with the severity of DR. The choroidoscleral interface was clearly identifiable throughout the 6-mm line scan in 19 of 24 controls (79%), 7 of 9 eyes with NPDR (78%), and 7 of 10 eyes with PDR (70%). This finding was consistent with previous studies on choroidal thickness in healthy and diseased states (19,20,24). However, only 9 of

14 eyes (64%) with DME had a clearly identifiable choroidoscleral interface throughout the 6-mm line scan. Failure to detect the choroidoscleral interface consistently means that the measurements of choroidal thickness throughout the 6-mm line scan in this group may be focally inaccurate. The cause is not clear, but it could be a result of hyperreflectivity of the incident light from the intraretinal fluid, leading to a shadowing effect of the deeper layers. Histological studies reveal an increase in thickness of the basement membrane of choroidal vessels (6) and choriocapillary “dropout”(10) in patients with DR. These changes may explain the alterations of choroidal morphological features in eyes with DR undergoing imaging with OCT. Nevertheless, these easily identifiable choroidal morphological features may have clinical utility in assessing the severity and/or predicting the progression of DR.

Evidence suggests that choroidal angiopathy in patients with DR may be present in association with retinopathy (9,20,26,27). The present study further enhances the understanding of choroidal angiopathy in DR by showing a reduction in the medium choroidal vessel layer and choriocapillaris layer thickness in eyes with PDR and DME compared with controls, which could be due to closure of the choriocapillaris in eyes with moderate to severe DR (9,28). In addition, choroidal thickness and vasculature measurements had no association with central retinal thickness in eyes with DR, suggesting that choroidal angiopathy may be independent of the retinopathy attributed to diabetes mellitus.

Although the choriocapillaris layer and the medium choroidal vessel layer could not be analyzed separately by using high-definition SD-OCT imaging, their distinction as a complex from the large choroidal vessel layer was achieved in this study with a strong interobserver correlation. Because the choriocapillaris layer forms only 5% to 10% of the choroid (29), delineation of this layer individually is difficult using the limited resolution of currently available SD-OCT devices. An individual delineation of this layer may be clinically relevant in diseases such as DR. Future imaging technologies using better resolution, a longer wavelength, and enface visualization of the choroidal vascular layers should allow for volumetric measurements of the choroid and visualization of its vasculature in refined detail (30-33), thereby improving our understanding of choroidal angiopathy in DR.

Limitations to this study include the unavailability of enhanced depth imaging scans. Enhanced depth imaging can provide a better view of the choroidoscleral interface by bringing the choroid closer to the zero-delay line (13) and, in this study, might have increased the percentage of eyes (especially in the DME group) in which the choroidoscleral interface could be accurately identified throughout the 6-mm line scan. To control for plausible discrepancies due to an obscure visualization of the choroidoscleral interface in eyes with DR, in particular those with DME, we used only 1 eye per patient with DR in which the choroidoscleral interface could be visualized for the morphological observations and subfoveal choroidal thickness and vasculature measurements that were performed in this study. Another limitation is the lack of treatment naïve patients in the DME and PDR groups. Studies suggest that panretinal photocoagulation alters choroidal blood flow in patients with PDR and that anti-VEGF therapy may affect choroidal thickness (34-37). Although we detected no effect of anti-VEGF therapy on the choroidal thickness and

vasculature measurements in eyes with DME in the present study, the number of eyes in this group was small.

In conclusion, this study demonstrated altered choroidal morphological features in eyes with DR and a significant thinning of the choroid overall and the combined thickness of the medium choroidal vessel layer and choriocapillaris layer specifically in eyes with PDR and DME compared with controls using SD-OCT. Further studies involving prospective correlation of increasing severity of DR with the morphological alteration of the choroid and changes in its vasculature may provide a better insight into the choroidal angiopathy associated with DR and its effect on the progression of disease.

## Acknowledgments

**Financial Support** This work was supported in part by a Research to Prevent Blindness Unrestricted grant to the New England Eye Center/Department of Ophthalmology -Tufts University School of Medicine, NIH contracts RO1-EY11289-23, RO1-EY13178-07, RO1-EY013516-07 and the Massachusetts Lions Eye Research Fund.

## REFERENCES

1. Antonetti DA, Klein R, Gardner TW. Diabetic retinopathy. *N Engl J Med*. 2012; 366(13):1227–1239. [PubMed: 22455417]
2. Shiragami C, Shiraga F, Matsuo T, Tsuchida Y, Ohtsuki H. Risk factors for diabetic choroidopathy in patients with diabetic retinopathy. *Graefes Arch Clin Exp Ophthalmol*. 2002; 240(6):436–442. [PubMed: 12107509]
3. Bartsch DU, Weinreb RN, Zinser G, Freeman WR. Confocal scanning infrared laser ophthalmoscopy for indocyanine green angiography. *Am J Ophthalmol*. 1995; 120(5):642–651. [PubMed: 7485366]
4. Dimitrova G, Kato S, Tamaki Y, et al. Choroidal circulation in diabetic patients. *Eye (Lond)*. 2001; 15(pt 5):602–607. [PubMed: 11702970]
5. Fukushima I, McLeod DS, Luty GA. Intrachoroidal microvascular abnormality: a previously unrecognized form of choroidal neovascularization. *Am J Ophthalmol*. 1997; 124(4):473–487. [PubMed: 9323938]
6. Hidayat AA, Fine BS. Diabetic choroidopathy: light and electronmicroscopic observations of seven cases. *Ophthalmology*. 1985; 92(4):512–522. [PubMed: 2582331]
7. Hirvelä H, Laatikainen L. Diabetic retinopathy in people aged 70 years or older: the Oulu Eye Study. *Br J Ophthalmol*. 1997; 81(3):214–217. [PubMed: 9135385]
8. Shiraki K, Moriwaki M, Kohno T, Yanagihara N, Miki T. Age-related scattered hypofluorescent spots on late-phase indocyanine green angiograms. *Int Ophthalmol*. 1999; 23(2):105–109. [PubMed: 11196117]
9. Schocket LS, Brucker AJ, Niknam RM, Grunwald JE, DuPont J, Brucker AJ. Foveolar choroidal hemodynamics in proliferative diabetic retinopathy. *Int Ophthalmol*. 2004; 25(2):89–94. [PubMed: 15290887]
10. Fryczkowski AW, Sato SE, Hodes BL. Changes in the diabetic choroidal vasculature: scanning electronmicroscopy findings. *Ann Ophthalmol*. 1988; 20(8):299–305. [PubMed: 3190107]
11. Huang D, Swanson EA, Lin CP, et al. Optical coherence tomography. *Science*. 1991; 254(5035):1178–1181. [PubMed: 1957169]
12. Wojtkowski M, Leitgeb R, Kowalczyk A, Bajraszewski T, Fercher AF. In vivo human retinal imaging by Fourier domain optical coherence tomography. *J Biomed Opt*. 2002; 7(3):457–463. [PubMed: 12175297]
13. Yeoh J, Rahman W, Chen F, et al. Choroidal imaging in inherited retinal disease using the technique of enhanced depth imaging optical coherence tomography. *Graefes Arch Clin Exp Ophthalmol*. 2010; 248(12):1719–1728. [PubMed: 20640437]



14. Chung SE, Kang SW, Lee JH, Kim YT. Choroidal thickness in polypoidal choroidal vasculopathy and exudative age-related macular degeneration. *Ophthalmology*. 2011; 118(5):840–845. [PubMed: 21211846]
15. Fujiwara T, Imamura Y, Margolis R, Slakter JS, Spaide RF. Enhanced depth imaging optical coherence tomography of the choroid in highly myopic eyes. *Am J Ophthalmol*. 2009; 148(3): 445–450. [PubMed: 19541286]
16. Imamura Y, Fujiwara T, Margolis R, Spaide RF. Enhanced depth imaging optical coherence tomography of the choroid in central serous chorioretinopathy. *Retina*. 2009; 29(10):1469–1473. [PubMed: 19898183]
17. Maruko I, Iida T, Sugano Y, Ojima A, Ogasawara M, Spaide RF. Subfoveal choroidal thickness after treatment of central serous chorioretinopathy. *Ophthalmology*. 2010; 117(9):1792–1799. [PubMed: 20472289]
18. Maruko I, Iida T, Sugano Y, et al. Subfoveal choroidal thickness after treatment of Vogt-Koyanagi-Harada disease. *Retina*. 2011; 31(3):510–517. [PubMed: 20948460]
19. Manjunath V, Goren J, Fujimoto JG, Duker JS. Analysis of choroidal thickness in age-related macular degeneration using spectral-domain optical coherence tomography. *Am J Ophthalmol*. 2011; 152(4):663–668. [PubMed: 21708378]
20. Regatieri CV, Branchini L, Carmody J, Fujimoto JG, Duker JS. Choroidal thickness in patients with diabetic retinopathy analyzed by spectral-domain optical coherence tomography. *Retina*. 2012; 32(3):563–568. [PubMed: 22374157]
21. Kur J, Newman EA, Chan-Ling T. Cellular and physiological mechanisms underlying blood flow regulation in the retina and choroid in health and disease. *Prog Retin Eye Res*. 2012; 31(5):377–406. [PubMed: 22580107]
22. Nickla DL, Wallman J. The multifunctional choroid. *Prog Retin Eye Res*. 2010; 29(2):144–168. [PubMed: 20044062]
23. Spraul CW, Lang GE, Lang GK, Grossniklaus HE. Morphometric changes of the choriocapillaris and the choroidal vasculature in eyes with advanced glaucomatous changes. *Vision Res*. 2002; 42(7):923–932. [PubMed: 11927356]
24. Manjunath V, Taha M, Fujimoto JG, Duker JS. Choroidal thickness in normal eyes measured using Cirrus HD optical coherence tomography. *Am J Ophthalmol*. 2010; 150(3):325.e1–329.e1. doi: 10.1016/j.ajo.2010.04.018. [PubMed: 20591395]
25. Branchini LA, Adhi M, Regatieri CV, et al. Analysis of choroidal morphologic features and vasculature in healthy eyes using spectral-domain optical coherence tomography [published online May 9, 2013]. *Ophthalmology*. doi:10.1016/j.optha.2013.01.066.
26. Weinberger D, Kramer M, Priel E, Gatton DD, Axer-Siegel R, Yassur Y. Indocyanine green angiographic findings in nonproliferative diabetic retinopathy. *Am J Ophthalmol*. 1998; 126(2): 238–247. [PubMed: 9727518]
27. Nagaoka T, Kitaya N, Sugawara R, et al. Alteration of choroidal circulation in the foveal region in patients with type 2 diabetes. *Br J Ophthalmol*. 2004; 88(8):1060–1063. [PubMed: 15258025]
28. Luty GA, Cao J, McLeod DS. Relationship of polymorphonuclear leukocytes to capillary dropout in the human diabetic choroid. *Am J Pathol*. 1997; 151(3):707–714. [PubMed: 9284819]
29. Ramrattan RS, van der Schaft TL, Mooy CM, de Bruijn WC, Mulder PG, de Jong PT. Morphometric analysis of Bruch's membrane, the choriocapillaris, and the choroid in aging. *Invest Ophthalmol Vis Sci*. 1994; 35(6):2857–2864. [PubMed: 8188481]
30. Unterhuber A, Povazay B, Hermann B, Sattmann H, Chavez-Pirson A, Drexler W. In vivo retinal optical coherence tomography at 1040 nm: enhanced penetration into the choroid. *Opt Express*. 2005; 13(9):3252–3258. [PubMed: 19495226]
31. Povazay B, Bizheva K, Hermann B, et al. Enhanced visualization of choroidal vessels using ultrahigh resolution ophthalmic OCT at 1050 nm. *Opt Express*. 2003; 11(17):1980–1986. [PubMed: 19466083]
32. Hirata M, Tsujikawa A, Matsumoto A, et al. Macular choroidal thickness and volume in normal subjects measured by swept-source optical coherence tomography. *Invest Ophthalmol Vis Sci*. 2011; 52(8):4971–4978. [PubMed: 21622704]

33. Srinivasan VJ, Adler DC, Chen Y, et al. Ultrahigh-speed optical coherence tomography for three-dimensional and en face imaging of the retina and optic nerve head. *Invest Ophthalmol Vis Sci*. 2008; 49(11):5103–5110. [PubMed: 18658089]
34. Takahashi A, Nagaoka T, Sato E, Yoshida A. Effect of panretinal photocoagulation on choroidal circulation in the foveal region in patients with severe diabetic retinopathy. *Br J Ophthalmol*. 2008; 92(10):1369–1373. [PubMed: 18662912]
35. Sayanagi K, Jo Y, Ikuno Y. Transient choroidal thinning after intravitreal bevacizumab injection for myopic choroidal neovascularization. *J Clin Exp Ophthalmol*. 2011; 2(165):1–5. doi: 10.4172/2155-9570.1000165.
36. Ellabban AA, Tsujikawa A, Ogino K, et al. Choroidal thickness after intravitreal ranibizumab injections for choroidal neovascularization. *Clin Ophthalmol*. 2012; 6:837–844. [PubMed: 22701085]
37. Branchini L, Regatieri C, Adhi M, et al. The effect of intravitreal anti-VEGF therapy on choroidal thickness in neovascular AMD using spectral-domain optical coherence tomography [published online March 14, 2013]. *JAMA Ophthalmol*. doi:10.1001/jamaophthalmol.2013.692.

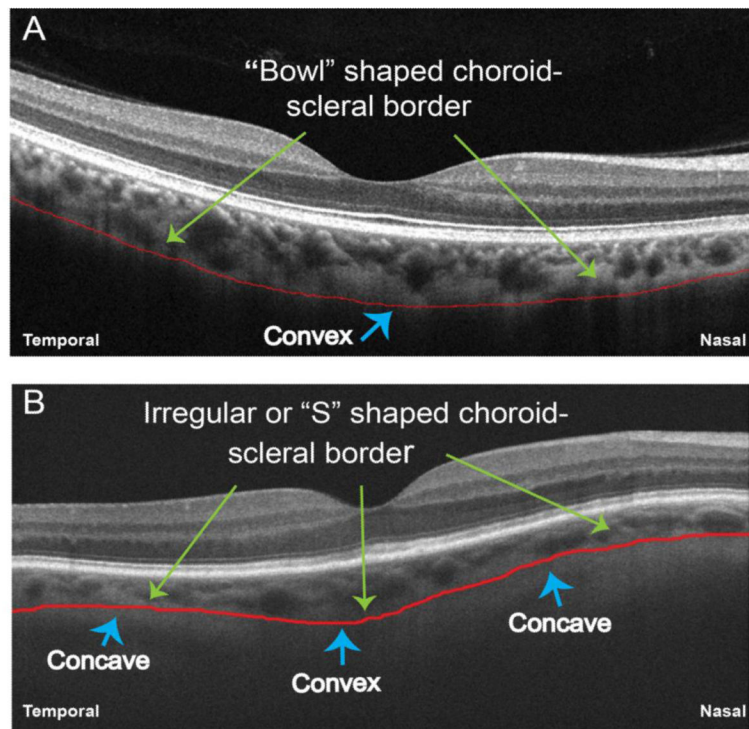


**Figure 1. Representative Optical Coherence Tomography Images Showing the Shape of the Choroidoscleral Interface**

A, A healthy eye has a convex or bowl shape to the choroidoscleral interface (red line). B, An eye with nonproliferative diabetic retinopathy has an irregular, concave-convex-concave or S shape to the choroidoscleral interface (red line).

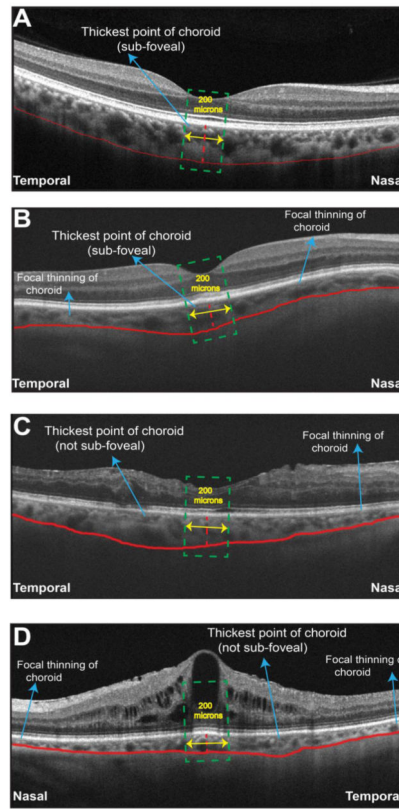


**Figure 2. Morphological Features of the Choroid in Healthy Eyes and Eyes With Diabetic Retinopathy (DR)**

A, Representative optical coherence tomography (OCT) image of a healthy eye with a thinner choroid nasally, much thicker beneath the fovea (falling within 200 $\mu$ m beneath the foveal center, green box), and temporal thinning. Red line represents the bowl shaped or convex contour to the choroidoscleral interface. B, Representative OCT image of an eye with nonproliferative diabetic retinopathy has an irregular or concave-convex-concave or S shape to the choroidoscleral interface (red line). The thickest point of the choroid is subfoveal (green box). Areas of focal choroidal thinning are seen. C, Representative OCT image of an eye with proliferative DR. An irregular or S shape to the choroidoscleral interface (red line) is seen. The thickest point of the choroid is temporally located. The nasal region shows focal thinning. D, Representative OCT image of an eye with diabetic macular edema. An irregular or S shape to the choroidoscleral interface (red line) is seen. The thickest point of the choroid is temporally located. The nasal and temporal regions show focal thinning.

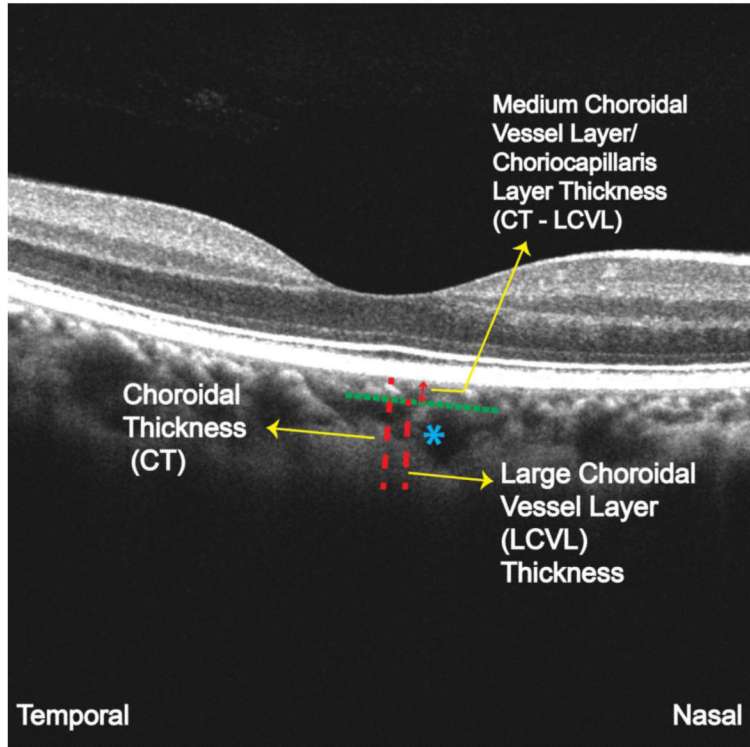


**Figure 3. Illustration of the Method Used to Analyze the Vascular Layers of the Choroid**  
The optical coherence tomography image of a healthy eye shows analysis of the choroidal vascular layers beneath the fovea. Blue asterisk represents the large choroidal vessel seen in the closest proximity to the fovea, and closest to the choroidoscleral interface, which was used for the large choroidal vessel layer (LCVL) measurements in this case. CT indicates choroidal thickness.

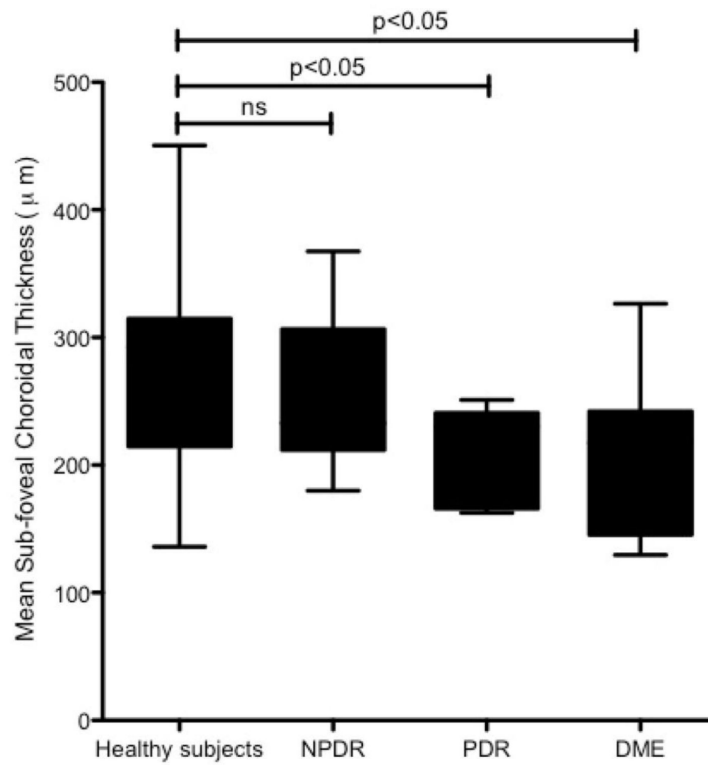


**Figure 4. Graph of the Mean Subfoveal Total Choroidal Thickness in Healthy Eyes and Eyes With Nonproliferative Diabetic Retinopathy (NPDR), Proliferative Diabetic Retinopathy (PDR), and Diabetic Macular Edema (DME)**

We found significant thinning of the choroid in eyes with PDR and DME compared with healthy eyes. Error bars represent the SEM. P values represent the results of the Tukey multiple comparisons test.

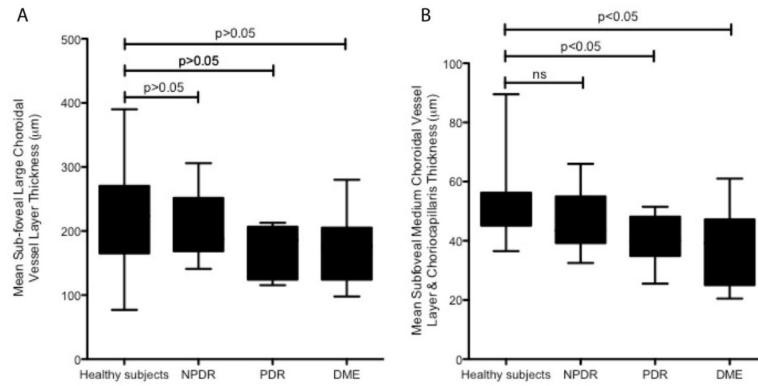


**Figure 5. Graphs of the Mean Subfoveal Choroidal Vessel Layer Thickness in Healthy Eyes and Eyes With Nonproliferative Diabetic Retinopathy (NPDR), Proliferative Diabetic Retinopathy (PDR), and Diabetic Macular Edema (DME)**

A, Mean (error bars represent SEM) subfoveal large choroidal vessel layer thickness. We found no significant difference in the mean subfoveal large choroidal vessel layer thickness between any groups. P values represent the results of the Tukey multiple comparisons test.

B, Mean (error bars represent SEM) combined subfoveal medium choroidal vessel layer and choriocapillaris layer thickness. A significant thinning of the mean subfoveal medium choroidal vessel layer and choriocapillaris layer thickness is seen in eyes with PDR and DME (but not in eyes with NPDR) compared with healthy eyes. P values represent the results of the Tukey multiple comparisons test.

**Table 1**  
**Characteristics of the Control Subjects and Patients With DR**

Abbreviations: CF 4', counting fingers at 4 feet; DME, diabetic macular edema; DR, diabetic retinopathy; NA, not applicable; NPDR, nonproliferative DR; PDR, proliferative DR; PRP, panretinal photocoagulation; VEGF, vascular endothelial growth factor.

	Healthy Subjects	NPDR patients	PDR patients	DME patients
Number of patients (eyes)	24 (24)	9 (9)	10 (10)	14 (14)
Age (years) Mean $\pm$ SD	45-70 62 $\pm$ 5.84	48-74 68 $\pm$ 6.73	42-73 68 $\pm$ 5.45	39-74 67 $\pm$ 6.02
Gender	Males – 11 (46%) Females – 13 (54%)	Males – 5 (55%) Females – 4 (45%)	Males – 4 (40%) Females – 6 (60%)	Males – 8 (57%) Females – 6 (43%)
Best-Corrected Visual Acuity (BCVA)	20/20	20/20 – 20/200	20/40 - CF 4'	20/25 - CF 4'
Prior Treatment with Focal Laser/PRP (number of eyes)	NA	NA	Yes (10)	Yes (14)
Prior Treatment with anti-VEGF agents (number of eyes)	NA	NA	No	Yes (8)



**Table 2**  
**Morphological Features of the Choroid in Control Subjects and Patients With DR**

Abbreviations: DME, diabetic macularedema; DR, diabetic retinopathy; NPDR, nonproliferative DR; PDR, proliferative DR.

<b>CHOROIDAL MORPHOLOGICAL FEATURE</b>	<b>Percentage of Healthy eyes with Choroidal Feature (n=24)</b>	<b>Percentage of NPDR eyes with Choroidal Feature (n=9)</b>	<b>Percentage of PDR eyes with Choroidal Feature (n=10)</b>	<b>Percentage of DME eyes with Choroidal Feature (n=14)</b>
1. "Bowl" shaped contour to the border of the choroid and sclera (1 point of inflection)	100%	11%	10%	7%
2. Choroidoscleral interface clearly identifiable throughout the 6mm line scan	79%	78%	70%	65%
3. Thickest point of choroid under the fovea	96%	22%	20%	14%
4. Focal of thinning of the choroid	0.0%	56%	40%	86%

**Table 3**  
**Choroidal Vessel Layer Thickness Measurements Relative to the Total Choroidal Thickness Beneath the Fovea in Control Subjects and Patients With DR**

Abbreviations: DME, diabetic macular edema; DR, diabetic retinopathy; NPDR, nonproliferative DR; PDR, proliferative DR . p values were obtained from the results of 1-way analysis of variance.

<b>MEAN CHOROIDAL VASCULAR MEASUREMENTS BENEATH THE FOVEA</b>					
<b>Vascular Parameter</b>	<b>Healthy eyes</b>	<b>NPDR eyes</b>	<b>PDR eyes</b>	<b>DME eyes</b>	<b>p-value</b>
Choroidal Thickness (μm)	276.4±13.4	252.9±20.27	209.6±12.42	211.6±17.05	0.007
Large Vessel Choroidal Layer Thickness (μm)	224.0±13.5	206.6±18.01	169.2±12.43	173.7±14.63	0.04
Medium Choroidal Vessel Layer & Choriocapillaris Layer Thickness (μm)	52.5±1.8	46.3±3.6	40.4±2.96	37.93±3.3	<0.001